Journal of The Korean Astronomical Society
40: 83 ∼ 89, 2007

CHEMICAL EVOLUTION IN VeLLOs

Jeong-Eun Lee
Department of Astronomy and Space Science, Sejong University, Seoul 143-747, Korea
E-mail: jelee@sejong.ac.kr
(Received November 16, 2007; Accepted December 6, 2007)

ABSTRACT

A new type of object called "Very Low Luminosity Objects (VeLLOs)" has been discovered by the Spitzer Space Telescope. VeLLOs might be substellar objects forming by accretion. However, some VeLLOs are associated with strong outflows, indicating the previous existence of massive accretion. The thermal history, which significantly affects the chemistry, between substellar objects with a continuous low accretion rate and objects in a quiescent phase after massive accretion (outburst) must be greatly different. In this study, the chemical evolution has been calculated in an episodic accretion model to show that CO and N_2H^+ have a relation different from starless cores or Class 0/I objects. Furthermore, the CO_2 ice feature at 15.2 μm will be a good tracer of the thermal process in VeLLOs.

Key words : ISM: astrochemistry – ISM: molecules – stars: formation

I. INTRODUCTION

The *Spitzer Space Telescope (SST)*, with its very high mid-infrared sensitivity, has revealed a new type of low-mass protostars called "Very Low Luminosity Objects (VeLLOs; e.g., Young et al. 2004). Defining the internal luminosity of a source, L_{int}, to be the total luminosity of the central protostar and circumstellar disk (if present), a VeLLO is defined to be an object embedded within a dense core that meets the criterion $L_{int} \leq 0.1$ $L_\odot$ (Di Francesco et al. 2007). VeLLOs are primarily being discovered in cores previously classified as starless based on observations with the *Infrared Astronomical Satellite (IRAS)* and the *Infrared Space Observatory (ISO)*. The three most well-studied VeLLOs to date are IRAM 04191 (André et al. 1999; Dunham et al. 2006), L1014 (Young et al. 2004; Crapsi et al. 2005; Bourke et al. 2005; Huard et al. 2006), and L1521F (Bourke et al. 2006), which show very different properties in molecular line observations despite their similar internal luminosities. IRAM 04191 (André et al. 1999; Belloche et al. 2002) and L1521F (Crapsi et al. 2004) show evidence for infall whereas L1014 does not (Crapsi et al. 2005). IRAM 04191 is associated with a well-collimated outflow (André et al. 1999); the other two are not, although at least L1014 and possibly L1521F feature weak, compact outflows (Bourke et al. 2005; Bourke et al. 2006).

The discovery of VeLLOs with *Spitzer* has put into question the picture of low-mass star formation as a continuous process of constant mass accretion at the standard rate of $\sim 2 \times 10^{-6}$ $M_\odot$ yr^{-1} (Shu, Adams, & Lizano 1987) through a single evolutionary sequence, the well-established class system progressing from Class 0 to III (Myers & Lada 1993, André et al. 1993). This standard accretion rate predicts a much higher luminosity than observed for VeLLOs; VeLLOs must feature some combination of a very low central mass and a very low accretion rate (e.g. Dunham et al. 2006). If the accretion continues at the current low rate to the very small central mass, it might not make a star. However, the accretion rate is not necessarily constant. For instance, FU Orionis (FU Ori) objects undergo outbursts (Bell et al. 1995 and references therein). Studies (Vorobyov & Basu 2005 and references therein) for the nature of the FU Ori variables suggest accretion bursts from the disk to the central star by the thermal instability of the disk.

Therefore, two potential explanations for the very low luminosities of VeLLOs are 1) proto-brown dwarfs, and 2) objects in a quiescent phase of the episodic accretion process. The former can be discriminated from the latter with studies of the chemistry since they involve vastly different thermal histories, which is crucial to the chemical evolution. The thermal history is especially important in interactions between gas and ice; ice evaporation and gas freeze-out from and onto grain surfaces, respectively, depend on the dust temperature (Lee et al. 2004). Proto-brown dwarfs, with their very low masses, will never experience a hot phase, whereas the outbursts of a cycle of episodic accretion, a short time period when the majority of the mass is dumped onto the central protostar, involve significant warming of the surrounding dust. The quiescent states between outbursts feature much colder dust temperatures. As a result, envelopes of proto-brown dwarfs will be similar to starless cores in their chemical distributions, while objects in a quiescent state of episodic accretion will show different chemical distributions from starless cores or normal, embedded Class 0/I objects.

IRAM 04191 may be undergoing episodic accretion since it features a strong outflow which predicts a higher accretion rate by two orders of magnitude than inferred from the internal luminosity of the source (André et al. 1999; Dunham et al. 2006). Further-

more, the N_2H^+ emission, observed with the Plateau de Bure Interferometer (PDBI) and the IRAM 30 m telescope, shows a hole in the center of the envelope (Belloche & André 2004). In general, N_2H^+ emission tends to peak towards the center of starless cores (Lee et al. 2003), but be deficient from the centers of Class 0/I sources due to destruction by CO as it evaporates (Lee et al. 2004). IRAM 04191 shows moderate CO depletion (Crapsi et al. 2004); Belloche & André (2004) suggest that freeze-out of N_2 in the high-density, inner envelope might result in the observed N_2H^+ hole. However, if freeze-out of N_2 is significant enough to explain this hole, there should be significantly more deuteration and depletion of CO than observed (Crapsi et al. 2004), similar to that seen in prestellar cores (Lee et al. 2003).

In this study, we model the chemical evolution in the process of episodic accretion to provide a possible explanation of the chemical distributions of CO and N_2H^+ in gas and to predict observable consequences in the CO_2 ice feature in VeLLOs such as IRAM 04191 that show strong evidence for undergoing such a process.

II. EPISODIC ACCRETION MODELS

We use the chemo-dynamical model developed by Lee et al. (2004). This model calculates the chemical evolution of a model core evolving from the prestellar stage through the embedded protostellar stages. The dynamical evolution is described by combining a sequence of Bonnor-Ebert spheres (Bonnor 1956, Ebert 1955) with the inside-out collapse model (Shu 1977), where the accretion rate from the envelope onto the star+disk system is constant. The model also includes the First Hydrostatic Core (FHSC) stage, which results from the first gravitational collapse of a dense molecular core and lasts until the core temperature reaches 2000 K and the dissociation of molecular hydrogen causes the second collapse (Boss 1993, Masunaga et al. 1998). The radius of the FHSC is about 5 AU, and the disk is not yet well developed at this stage. As a result, the accretion luminosity arising from accretion onto the FHSC is not significant. The evolution of the central luminosity follows that adopted by Young & Evans (2005), who incorporated the evolution of an unresolved disk and stellar photosphere into the central luminosity. This luminosity is proportional to the accretion luminosity arising from envelope accretion following the inside-out collapse model (see Young & Evans 2005 for details).

In this study, we assume that the accretion from the envelope to the disk is constant, but the accretion from the disk to the star is episodic. Thus, the envelope density structure is identical to that of the inside-out collapse model, but the internal luminosity is changed by the episodic accretion process. The initial mass of the model core, with an effective sound speed of 0.27 km s^{-1} and outer radius of 6200 AU, is 1 $M_\odot$ (Equation 1 of Young & Evans 2005). The episodic accretion is assumed to begin after the FHSC phase, which lasts for 2×10^4 years.

The dust temperature profile at each time step is calculated with the one dimensional continuum radiative transfer code DUSTY (Ivezić et al. 1999), using as input the density profile from the inside-out collapse model. The input internal radiation field at each time step is calculated by the model of Young & Evans (2005) with their standard parameters of $\eta_D = 0.75$, $\eta_* = 0.5$, and $\tau_{max} = 10$ (see Young & Evans 2005 for a detailed explanation of these parameters) combined with our prescription for episodic accretion. In this prescription, accretion bursts 10 times more massive than normal ($\dot{M} \sim 5 \times 10^{-6}$ $M_\odot$ yr^{-1}) occur during 10^3 years every 10^4 years. For the 9×10^3 years between the accretion burst events, the accretion from the disk to the star is decreased by a factor of 100. Vorobyov & Basu (2005) have showed that $0.01 \sim 0.05$ $M_\odot$ is accreted from the disk to the central source with the accretion rate of $(1 \sim 10) \times 10^{-4}$ $M_\odot$ yr^{-1} during a burst, and the duration of the intervening quiescent accretion phase is $(1 \sim 3) \times 10^3$ years for $\dot{M} = (1 - 10) \times 10^{-7}$ $M_\odot$ yr^{-1}. According to their calculations and for the accretion rates in the burst and quiescent phases in this model, which are about an order of magnitude smaller than the rates of Vorobyov & Basu (2005), we adopt the timescales of 10^3 and 10^4 years in the two phases, respectively, and these timescales are consistent with the estimated from HL Tauri by Lin et al. (1994).

We calculate the radiative transfer independently at each time step since the dust temperature reaches a new equilibrium essentially instantly compared to the length of our time step. For example, one silicate grain with a radius of 0.1 μm and a temperature of 100 K will cool down to 10 K within one second if the heating source suddenly disappears (Draine & Anderson 1985). Following Young & Evans (2005), the envelope is heated externally by the Black-Draine Interstellar Radiation Field (ISRF) (Evans et al. 2001) attenuated by a visual extinction of 0.5 mag. Also following Young & Evans, we used the dust model of Ossenkopf & Henning (1994) appropriate for thin ice mantles after 10^5 years of coagulation at a gas density of 10^6 cm^{-3} (OH5 dust).

Fig. 1a shows the evolution of the total internal luminosity in the model, and Fig. 1b shows the temperature evolution of a few infalling grid points. As seen in this figure, the temperature that an infalling gas parcel experiences peaks at the time step of each massive accretion and is lowered significantly during the quiescent states. Betwen 4 and 5.5×10^4 years, the luminosity and temperature increase steeply with time even in the quiescent phase because of the transition from the FHSC to Class 0, which occurs from 2×10^4 years until 5.5×10^4 years. This transition timescale is the same as that used in Lee et al. (2004), but much longer than the 100 years assumed by Young & Evans

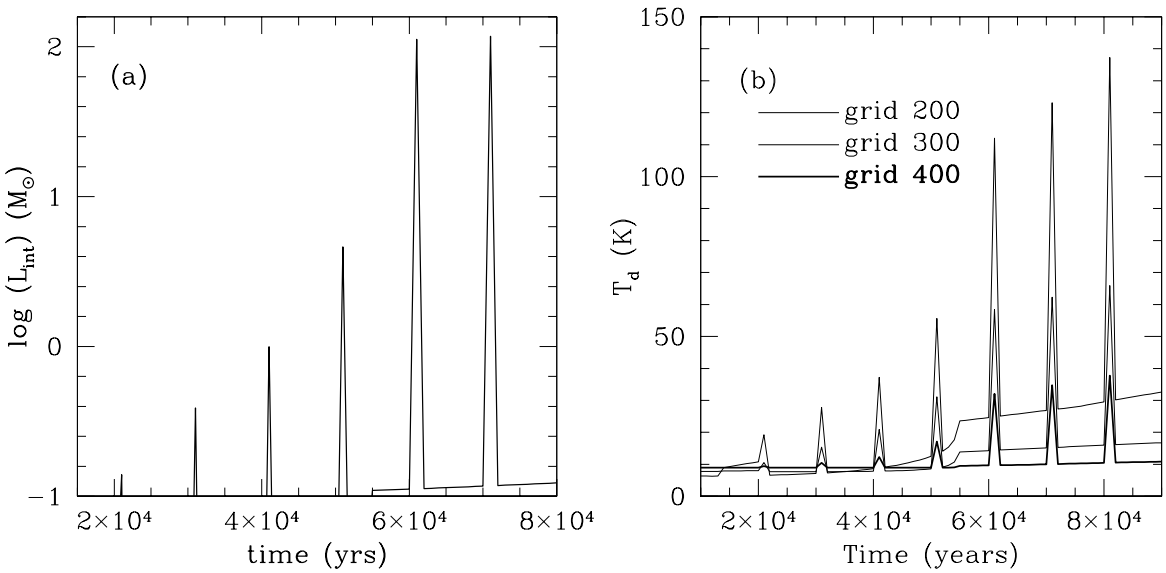

Fig. 1.— (a) Evolution of the internal luminosity in the episodic accretion model. Outburts (massive accretion events) occur every 10^4 years for 10^3 years after the FHSC phase, which lasts until 2×10^4 years. (b)Evolution of dust temperatures in infalling gas parcels. Grids 200, 300, and 400 are initially located at the radii of 0.0023, 0.0055, and 0.0124 pc, respectively.

(2005).

The evolution of the spectral energy distribution (SED) around 5×10^4 years is presented in Fig. 2. An accretion burst occurred at 5.1×10^4 years, after which a quiescent state continues until the next burst 10^4 years later. The accretion luminosity powered in the burst phase at 5.1×10^4 years is about 5 $L_\odot$, whereas the accretion luminosities at 5.0 and 5.4 $\times 10^4$ years are about 0.004 and 0.02 $L_\odot$, respectively. The model SED at 5.4×10^4 years fits well the observed SED of IRAM 04191. The total luminosity in the model is about 0.09 $L_\odot$, where the luminosity arising from heating by the ISRF ($\sim$ 0.07 $L_\odot$) is larger than the internal luminosity ($\sim$ 0.02 $L_\odot$). This result is not very consistent with that of Dunham et al. (2006), who found that the internal luminosity must be greater than 0.04 $L_\odot$. However, the density profile and ISRF in their model are significantly different from ours, making it hard to directly compare the two results.

The density and dust temperature profiles are shown in Fig. 3 at the same time steps shown for the SEDs in Fig. 2. The infall radius is 0.014 pc (2800 AU) when the accretion burst occurs at 5.1×10^4. The density at the infall radius is about 2×10^5 cm^{-3}. The density profile has the power law index of $\sim$ 1.5 and 2.0 inside and outside the infall radius, respectively. Except for the accretion burst phase, the dust temperature is below the CO evaporation temperature ($\sim$ 20 K) at almost all radii.

III. CHEMICAL EVOLUTION IN A CYCLE OF EPISODIC ACCRETION

In prestellar cores, which are very evolved starless cores, carbon-bearing molecules such as CS and CO are readily frozen-out onto grain surfaces (Bergin & Langer 1997, Aikawa et al. 2001, Lee et al. 2003, Lee et al. 2004). In contrast, nitrogen-bearing molecules such as N_2H^+ and NH_3 are considered good tracers of (column) density in cold, dense cores since N_2, the parent molecule of N_2H^+ and NH_3, has a long formation timescale such that it becomes abundant later in the core evolution. Therefore, the comparison between CO and N_2H^+ abundances is a good indicator of the physical properties of a dense core.

The low binding energy of N_2 on grain surfaces has also been suggested as an explanation for the long-lived molecules in the cold regions (Lee et al. 2004). However, Öberg et al. (2005) showed that the binding energy of N_2 on grain surfaces is not different from that of CO. The high abundance of N_2H^+ in the cold, dense regions may be due to the replenishment of N_2 through the interactions between N_2H^+ and grains since N_2H^+ recombines with electrons on the grain surfaces. The significant depletion of CO and electrons, the principal destroyers of N_2H^+ in the gas phase, is another explanation for the high abundance of N_2H^+ in these cold, dense regions.

We updated the chemical network used in Lee et al. (2004) to include recent results on the N_2H^+ chemistry,

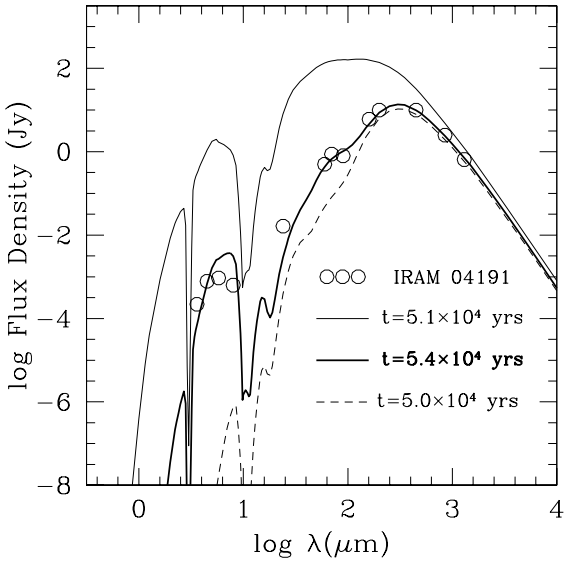

Fig. 2.— Evolution of SED in the episodic accretion model. The dashed, thick solid, and thin solid lines represent the SEDs 10^3 years before, 3×10^3 years after, and during the outburst at 5.1×10^3 years, respectively.

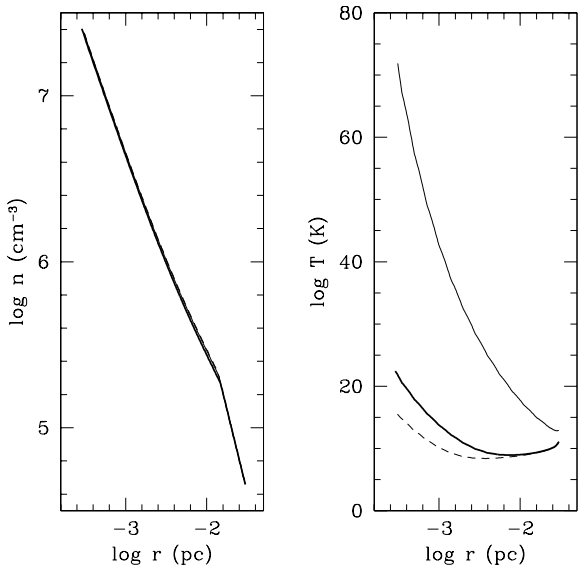

Fig. 3.— Evolution of density and temperature profiles. Time steps for different line styles are the same as those in Fig. 2. The density structure in the envelope does not change much for 4×10^3 years, but the dust temperature varies significantly over the episodic accretion event. During the outburst, the dust temperature jumps above the CO evaporation temperature at radii smaller than about 0.006 pc ($\sim$ 1300 AU). During the quiescent states, the dust temperature is below the CO evaporation temperature ($\sim$ 20 K).

including a new binding energy of N_2 identical to that of CO (Öberg et al. 2005) and new rates of dissociative recombination of N_2H^+ with electrons (Geppert et al. 2004). The initial abundances of other species are the same as those in Table 3 of Lee et al. (2004). Bare silicate grains were assumed for binding energies of molecules.

Fig. 4 presents the evolution of the CO abundance in gas and ice at the time steps 10^3 years before, during, and 3 and 5×10^3 years after the accretion burst at 5.1×10^4 years since the model SED at 5.4×10^4 years fits the observations of IRAM 04191 reasonably well. 10^3 years before the accretion burst, CO is frozen-out onto grain surfaces and depleted from the gas at most radii except around the CO evaporation radius, inside which the dust temperature is higher than the CO evaporation temperature, developed by the previous accretion burst at 4.1×10^4 years. During the burst phase, the CO evaporation radius jumps to a much larger radius due to the significant increase in accretion luminosity. Once the burst phase ends and the core makes the transition back to the quiescent phase, the accretion luminosity, and therefore the temperature, decreases greatly. CO is then gradually frozen back out of the gas and onto the grain surfaces.

The evolution of the N_2H^+ abundance is shown in Fig. 5. Before the accretion burst at 5.1×10^4 years, the N_2H^+ abundance peaks at a rather large radius and decreases inward. (The sharp drop of the N_2H^+ abundance at the edge of the model core results from the dissociative recombination of N_2H^+ with electrons.) At radii of 0.002 pc (log r~ -2.7) and 0.0008 pc (log r~ -3.1), the bumps of N_2H^+ are caused by the dips of CO at these radii. The N_2H^+ abundance decreases at radii smaller than 0.0008 pc even though CO is depleted here. N_2H^+ forms mainly by the reaction between N_2 and H_3^+, which is destroyed by CO. As mentioned above, the evaporation temperature of N_2 is the same as that of CO, i.e., $\sim$20 K. Therefore, at the radii smaller than 0.0008 pc where the dust temperature is lower than $\sim$ 20 K, and the density is greater than 10^6 cm^{-3}, the significant freeze-out of N_2 causes the low abundance of N_2H^+. During the burst phase, the N_2H^+ abundance drops significantly at radii smaller than the CO evaporation radius since CO destroys N_2H^+. In the quiescent states 3, 5, and 8×10^3 years after the burst, N_2H^+ slowly increases at small radii as CO is frozen-out onto the grain surfaces.

IV. DISCUSSION

Most VeLLOs were classified as starless core before *Spitzer* observations, and they showed wide vari-

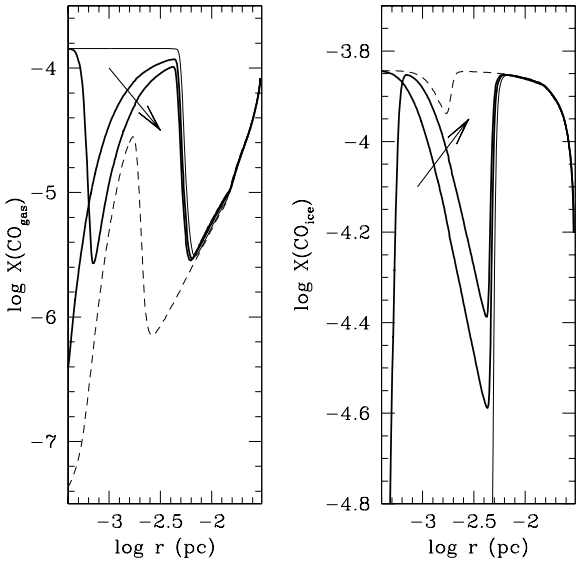

Fig. 4.— Evolution of the abundance profile of CO in gas and ice. Time steps for different line styles are the same as those in Fig. 2 except for one more thick solid line 5×10^3 years after the outburst event. Before the outburst (dashed line), the CO abundance profiles in gas and ice have a peak and a dip, respectively, at ~ 0.002 pc, which are vestiges of the prior outburst at 4.1×10^4 years. During the outburst (thin solid line), CO evaporates, and thus, the CO abundance in gas reaches the maximum at radii smaller than 0.006 pc. For the CO ice, the opposite happens, i.e., the abundance drops sharply at 0.006 pc. The arrow in each panel indicates the evolution of the abundance profile with time after the massive accretion event. That is, CO is gradually frozen-out onto grain surfaces to become depleted in gas and abundant in ice with time.

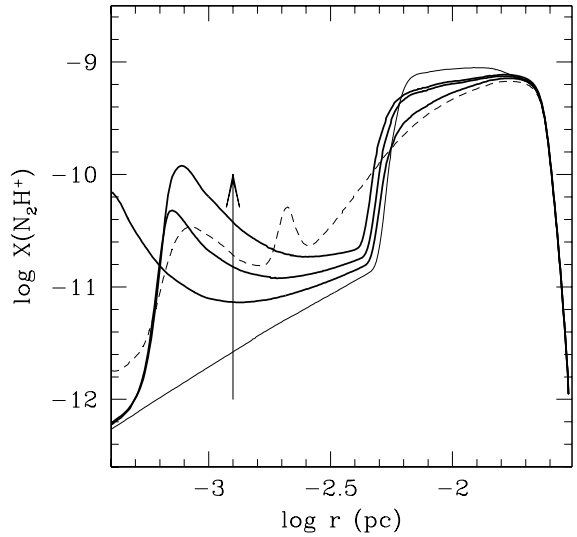

Fig. 5.— Evolution of the abundance profile of N_2H^+. The time steps for different line types are the same as those in previous figures, but the thick solid lines show the abundance evolution 3, 5, and 8 $\times 10^3$ years after the outburst as indicated with the arrow. The bumps shown in the dashed line (before the outburst) are vestiges of the previous outburst that occurred at 4.1×10^4 years. During the outburst (thin solid line), N_2H^+ is destroyed by CO inside the CO evaporation radius, so its abundance drops sharply at radii smaller than the CO evaporation radius. In the quiescent phase (thick solid lines), the N_2H^+ abundance gradually increases as CO is frozen out onto grain surfaces.

ation in chemical and physical properties. For instance, IRAM 04191 (André et al. 1999) and L673-7 (M. Dunham 2007, private communication) have well-collimated molecular outflows, but no molecular outflow has been detected in L1521F even though its *Spitzer* IRAC images show a compact bipolar scattered emission nebula (Bourke et al. 2006). L1014 features a very compact outflow detected with the Submillimeter Array (Bourke 2005). In chemical properties, IRAM 04191 and L1014 are similar with moderate CO depletion but different in their N_2H^+ emission, which peaks at the center of L1014 but shows a hole at the center of IRAM 04191. L1521F, which was believed to be a highly evolved starless core (Crapsi et al. 2004), shows significant CO depletion and centrally peaked N_2H^+ emission. Before the *Spitzer* observations, this variation in chemical properties was believed to arise from an as-of-yet incompletely understood evolutionary sequence of starless cores. The discovery of the VeLLOs has cast doubt on our understanding of the continuous and unique sequence of star formation consisting of the evolution of a starless core into a prestellar core followed by the formation of a Class 0 object that then evolves through the Class system.

The sources without strong outflows might be in the final accretion phase of substellar objects or in the FHSC stage (Omukai et al. 2007). On the other hand, VeLLOs with strong, well-collimated outflows such as IRAM 04191 are hard to understand since the outflow suggests a much higher accretion luminosity than the observed internal luminosity of the source. A possible explanation for such objects is episodic accretion. In this picture, VeLLOs are objects in quiescent phases of a cycle of episodic mass accretion. The strong outflows observed can be generated during accretion bursts that occurred prior to the current quiescent phase. These two processes predict vastly different thermal histories, which can be discriminated by their different predictions for the chemical evolution of the core. Observations probing these different predictions are challenging, however, since high spatial resolution is required to resolve the regions most affected by the different ther-

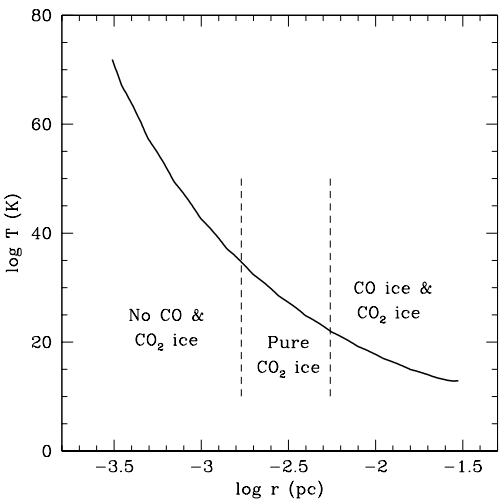

Fig. 6.— Distribution of CO and CO_2 ices depending on the temperature distribution developed by the outburst at 5.1×10^4 years.

mal histories. In addition, observations of ice features require high sensitivities due to the very low luminosities of the central source.

As seen in the previous section, the relation between CO and N_2H^+ abundances in an object featuring episodic accretion is different from that of starless cores or hot corinos, where CO and N_2H^+ have an anti-correlation. In the quiescent phase after an outburst, both CO and N_2H^+ have not had enough time to reach chemical equilibrium. As a result, CO can be less depleted and N_2H^+ more depleted compared to a core forming a proto-brown dwarf with a similar central luminosity to IRAM 04191.

CO in ice can also be a discriminator since CO ice features from VeLLOs in a quiescent phase of episodic accretion will be weaker than those in proto-brown dwarfs. Additionally, the CO_2 ice features can also be very important tracers of the thermal history of VeLLOs. The CO_2 15.2 μm bending mode has been detected toward massive star forming regions (Gerakines et al. 1999), low mass star forming cores (Pontoppidan et al. 2007) and even dark molecular clouds (Knez et al. 2005). The formation process of the CO_2 ice is controversial, but it must form on grain surfaces since the abundance of the CO_2 gas in dark clouds is too low (10^{-9}, Bergin et al. 1995) to explain the observed CO_2 ice features. CO_2 ices are found both in water- and CO-rich grain surfaces. Therefore, the CO_2 ice likely forms on grain surfaces by the reactions between CO frozen-out from gas and OH or O photodissociated from water or CO in ice. The photodissociation of water or CO on grain surfaces, especially in low mas star forming cores, can occur by the cosmic ray induced UV photons. As a result, the timescale of the formation of CO_2 on grain surfaces must be long ($> 10^4$ years in the density of 10^5 cm^{-3}, Pontoppidan et al. 2007.)

The evaporation temperature of the CO_2 ice is about 35 K, higher and lower than the CO (20 K) and H_2O (100 K) evaporation temperatures, respectively. In outburst phases of episodic accretion, the dust temperature can rise above the CO_2 evaporation temperature at some inner radii. There is also a range of radii where the dust temperature is between the CO and CO_2 evaporation temperatures, so CO_2 remains on grain surfaces while CO evaporates. In this range, CO_2 will produce the double-peaked feature indicative of pure CO_2 ice (Pontoppidan et al. 2007). In the following quiescent phase, CO will be gradually frozen-out as seen above, and thus, combined with the long formation timescale of CO_2, the solid CO_2 abundance profile developed in the outburst phase will not change greatly. As a result, we expect that objects in quiescent stages of episodic accretion will have a weaker solid CO_2 feature (if CO_2 evaporates up to a large radius) but a stronger pure CO_2 feature (if the range of CO_2 evaporation is not large) compared to substellar objects. Fig. 6 shows the temperature profile during an outburst with marks for the CO and CO_2 ice mixture. However, if the VeLLOs are proto-brown dwarfs, which never raise the dust temperature above the CO and CO_2 evaporation temperatures in the majority of their envelopes, then the solid CO_2 feature will be strong as seen toward background sources without a strong pure CO_2 component (Knez et al. 2005). Therefore, the CO_2 ice feature as well as the abundance distribution of CO and N_2H^+ in gas can be good tracers of the formation processes of VeLLOs.

ACKNOWLEDGEMENTS

This work was supported by the faculty research fund of Sejong University in 2007. We are very grateful to Mike Dunham and Neal Evans for valuable comments.

REFERENCES

Aikawa, Y., Ohashi, N., Inutsuka, S.-I., Herbst, E., & Takakuwa, S., 2001, Molecular Evolution in Collapsing Prestellar Cores, ApJ, 552, 639

André, P., Ward-Thompson, D., & Barsony, M., 1993, Submillimeter continuum observations of Rho Ophiuchi A - The candidate protostar VLA 1623 and prestellar clumps, ApJ, 406, 122

André, P., Motte, F., & Bacmann, A., 1999., Discovery of an Extremely Young Accreting Protostar in Taurus, ApJ, 513, L57

Bergin, E. A., Langer, W. D., & Goldsmith, P. F., 1995, Gas-phase chemistry in dense interstellar clouds including grain surface molecular depletion and desorption, ApJ, 441, 222

Bell, K. R., Lin, D. N. C., Hartmann, L. W., & Kenyon, S. J., 1995, The FU Orionis outburst as a thermal accretion event: Observational constraints for protostellar disk models, ApJ, 444, 376

Belloche, A., André, P., Despois, D., & Blinder, S., 2002, Molecular line study of the very young protostar IRAM 04191 in Taurus: infall, rotation, and outflow, A&A, 393, 927

Belloche, A. & André, P., 2004, Disappearance of N_2H^+ from the gas phase in the class 0 protostar IRAM 04191, A&A, 419, L35

Bergin, E. A. & Langer, W. D., 1997, Chemical Evolution in Preprotostellar and Protostellar Cores, ApJ, 486, 316

Bonnor, W. B., 1956, Boyle's Law and gravitational instability, MNRAS, 116, 351

Boss, A. P., 1993, Collapse and fragmentation of molecular cloud cores. I - Moderately centrally condensed cores, ApJ, 410, 157

Bourke, T. L., Crapsi, A., Myers, P. C., Evans, N. J. II, Wilner, D. J., Huard, T. L., Jørgensen, J. K., & Young, C. H., 2005, Discovery of a Low-Mass Bipolar Molecular Outflow from L1014-IRS with the Submillimeter Array, ApJ, 633, L129

Bourke, T. L., et al., 2006, The Spitzer c2d Survey of Nearby Dense Cores. II. Discovery of a Low-Luminosity Object in the "Evolved Starless Core" L1521F, ApJ, 649, L37

Crapsi, A., Caselli, P., Walmsley, C. M., Tafalla, M., Lee, C. W., Bourke, T. L., & Myers, P. C., 2004, Observations of L1521F: A highly evolved starless core, A&A, 420, 957

Crapsi, A., et al., 2005, Dynamical and chemical properties of the "starless" core L1014, A&A, 439, 1023

Di Francesco, J., Evans. N. J., II, Caselli, P., Myers, P. C., Shirley, Y., Aikawa, Y., & Tafalla, M., 2007, in Protostars and Planets V, ed. B. Reipurth, D. Jewitt, & K. Keil (Tucson: Univ. Arizona Press)

Draine, B. T. & Anderson, N., 1985, Temperature fluctuations and infrared emission from interstellar grains, ApJ, 292, 494

Dunham, M. M., et al., 2006, The Spitzer c2d Survey of Nearby Dense Cores. I. First Direct Detection of the Embedded Source in IRAM 04191+1522, ApJ, 651, 945

Ebert, R., 1955, Uber die Verdichtung von H I-Gebieten. Mit 5 Textabbildungen, Z. Astrophys., 37, 217

Evans, N. J. II, Rawlings, J. M. C., Shirley, Y., & Mundy, L. G., 2001, Tracing the Mass during Low-Mass Star Formation. II. Modeling the Submillimeter Emission from Preprotostellar Cores, ApJ, 557, 193

Geppert, W. D., Thomas, R., Semaniak, J., Ehlerding, A., Millar, T., Österdahl, F., af Ugglas, M., Djurić, N., Paál, A., & Larsson, M., 2004, Dissociative Recombination of N_2H^+: Evidence for Fracture of the NN Bond, ApJ, 609, 459

Gerakines, P. A., Whittet, D. C. B., Ehrenfreund, P., Boogert, A. C. A., Tielens, A. G. G. M., Schutte, W. A., Chiar, J. E., v an Dishoeck, E. F., Prusti, T., Helmich, F. P., & de Graauw, T., 1999, Observations of Solid Carbon Dioxide in Molecular Clouds with the Infrared Space Observatory, ApJ, 522, 357

Huard, T. L., et al., 2006, Deep Near-Infrared Observations of L1014: Revealing the Nature of the Core and Its Embedded Source, ApJ, 640, 391

Ivezić, Ž., Nenkova, M., & Elitzur, M., 1999, User Manual for DUSTY, astro-ph/9910475

Knez, C., Boogert, A. C. A., Pontoppidan, K. M., Kessler-Silacci, J., van Dishoeck, E. F., Evans, N. J. II, Augereau, J.-C., Blake, G. A., & Lahuis, F., 2005, Spitzer Mid-Infrared Spectroscopy of Ices toward Extincted Background Stars, ApJ, 635, L145

Lee, J.-E., Evans, N. J., II, Shirley, Y. L., & Tatematsu, K., 2003, Chemistry and Dynamics in Pre-protostellar Cores, ApJ, 583, 789

Lee, J. -E., Bergin, E. A., & Evans, N. J. II, 2004, Evolution of Chemistry and Molecular Line Profiles during Protostellar Collapse, ApJ, 617, 360

Lin, D. N. C., Hayashi, M., Bell, K. R., & Ohashi, N., 1994, Is HL Tauri and FU Orionis system in quiescence?, ApJ, 435, 821

Masunaga, H., Miyama, S. M., & Inutsuka, S. -I., 1998, A Radiation Hydrodynamic Model for Protostellar Collapse. I. The First Collapse, ApJ, 495, 346

Öberg K. I., van Broekhuizen, F., Fraser, H. J., Bisschop, S. E., van Dishoeck, E. F., & Schlemmer, S., 2005, Competition between CO and N_2 Desorption from Interstellar Ices, ApJ, 621, 33

Myers, P. C. & Ladd, E. F., 1993, Bolometric temperatures of young stellar objects, ApJ, 413, L47

Omukai, K., 2007, Observational Characteristics of the First Protostellar Cores, PASJ, 59, 589

Ossenkopf V. & Henning Th., 1994, Dust opacities for protostellar cores, A&A, 291, 943

Pontoppidan, K. M, Boogert, A. C. A., Fraser, H. J., van Dishoeck, E. F., Blake, G. A., Lahuis, F., Öberg, K. I., Evans, N. J.,II, & Salyk, C., 2007, The c2d Spitzer spectroscopic survey of ices around low-mass young stellar objects II: CO2, ApJ, in press

Shu, F. H., 1977, Self-similar collapse of isothermal spheres and star formation, ApJ, 214, 488

Shu, F. H., Adams, F. C., & Lizano, S., 1987, Star formation in molecular clouds - Observation and theory, ARA&A, 25, 23

Vorobyov, E. I. & Basu, S., 2005, The Origin of Episodic Accretion Bursts in the Early Stages of Star Formation, ApJL, 633, 137

Young, C. H., et al., 2004, Infrared Properties of Radio-selected Submillimeter Galaxies in the Spitzer First Look Survey Verification Field, ApJS, 154, 396

Young, C. H., & Evans, N. J., 2005, Evolutionary Signatures in the Formation of Low-Mass Protostars, ApJ, 627, 293